Hindawi
International Journal of Computer Games Technology
Volume 2021, Article ID 2914190, 10 pages
https://doi.org/10.1155/2021/2914190

Research Article

Trajectory Tracking of Autonomous Ground Vehicles with Actuator Dead Zones

Pengfei Zhang, Qiyuan Chen, and Tingting Yang

School of Engineering, Huzhou University, Huzhou 313000, China

Correspondence should be addressed to Tingting Yang; 02820@zjhu.edu.cn

Received 10 August 2021; Revised 15 November 2021; Accepted 10 December 2021; Published 24 December 2021

Academic Editor: Yiyu Cai

This paper investigates the trajectory tracking problem of autonomous ground vehicles (AGVs). The dynamics considered feature external disturbances, model uncertainties, and actuator dead zones. First, a novel time-varying yaw guidance law is proposed based on the line of sight method. By a state transformation, the AGV is proved to realize trajectory tracking control under the premise of eliminating guidance deviation. Second, a fixed time dead zone compensation control method is introduced to ensure the yaw angle tracking of the presented guidance. Furthermore, an improved fixed-time disturbance observer is proposed to compensate for the influence of the actuator dead zone on disturbance observation. Finally, the trajectory tracking control strategy is designed, and simulation comparison shows the effectiveness of the compensate method. The CarSim–MATLAB cosimulation shows that the proposed control strategy effectively makes the AGV follow the reference trajectory.

1. Introduction

Trajectory tracking control of autonomous ground vehicles (AGVs) plays an essential role in domestic and industrial use for increasing safety, accuracy, and efficiency demands, such as self-guiding uncrewed driving vehicles, platform supplying, and minesweeping [1]. Critical to the trajectory tracking problem of an AGV is its capability for accurate and reliable control to follow the desired trajectory by the planner [2]. The high dynamic nonlinearity, uncertainties and disturbances, and the mechanical limitations of the vehicle itself make the AGV trajectory tracking control challenging.

Various research results exist in the literature. Some existing works investigate the trajectory tracking problem of AGVs utilizing the kinematic model [3, 4]. However, the driving condition may be limited without reckoning the dynamics model. For this reason, the trajectory tracking control problem of a class of autonomous vehicles is investigated with parametric uncertainties, external disturbances, and overactuated features by introducing a novel adaptive hierarchical control framework with the linear matrix inequality technique [5]. Then, an augmented state variable and a nonlinear observer are trained to design a torque overlay-base robust steering wheel angle control with the backstepping method [6]. A robust H_{∞} dynamic output-feedback controller is designed to control the vehicle motion without using the lateral velocity information [7]. Besides, an accurate and efficient clothoid approximation approach is presented using Bezier curves [8]. A model predictive control law incorporating neural-dynamic optimization is introduced [9].

Compared with the above approaches, the finite-time control method has faster convergence speed, better disturbance rejection property, and better robustness against uncertainties [10]. Further, a fixed-time control method can guarantee global exponential convergence within a designated time independent of the initial conditions [11]. Thus, a fixed-time control scheme of AGVs might be of great significance. Apart from that, the actuator dead-zones with uncertainty issues have seldom been investigated in the trajectory tracking control design. Due to the mechanical limitations of the vehicle itself, dead zones in yaw actuators should be considered. Dead zones are commonly observed in servo valves or DC servo motors of AGVs but are not discussed in the above papers [12, 13]. When the control input

falls in the dead zone, the actuator will have no output signal, resulting in steady-state errors and degraded performance in the system. How to address the actuator dead-zone issue in the fixed-time trajectory tracking control problem of AGVs still requires extensive research.

The trajectory tracking control law should achieve disturbance rejection to enhance accuracy and reliability. The LQR technique investigates a hierarchical adaptive trajectory tracking control for autonomous vehicles [14]. A compensation method combining NTSM and ARDC is presented [4]. A kinematic MPC handling the disruptions on road curvature and a PID feedback control of yaw rate rejecting uncertainties and modeling errors are designed to follow the reference trajectory [15]. The intelligent control method of interactive control paradigm-based robust lateral stability controller design for autonomous automobile trajectory tracking with uncertain disturbance is proposed [16]. Above all, the EKF, LQR, and MPC are usually simplified with limited available model parameters. However, time-varying and nonlinear terms always exist, which cannot be regarded as white Gaussian noise. The intelligent control method generally depends on experience and enough off-line training. Although the ARDC method may effectively solve the uncertain systems and be easy to implement, observer error convergence's settling time is inaccurate. The DOBC method is a good option for rejecting disturbances in such a case. Mainly, a fixed-time observer can estimate the perturbance within a given settling time [17]. However, since the existence of dead zones, it is difficult to obtain the complete control signal. Thus, existing fixed/finite-time observers cannot directly be applied in the tracking control problem.

Motivated by the above observations, this paper is aimed at giving a fixed-time observer-based control method, rendering the AGVs with yaw actuator dead zones to follow the reference trajectory. To this end, time-varying yaw guidance and corresponding state transformation are introduced to convert trajectory tracking control into a simple yaw angle tracking problem. A fixed-time observer-based control scheme solving the actuator dead-zones is constructed for the transformed system, whose dwell times are independent of the initial conditions. The main contributions of this paper are threefold:

(1) A novel time-varying yaw guidance law is proposed based on the line of sight method, which can overcome the undesired terms involved in the error dynamics

(2) Uncertainties, external disturbances, and dead zones are simultaneously considered in the tracking control problem, making the designed controller robust to more extensive and challenging. Note that there is seldom any previous work addressing the control issues in one controller

(3) Based on fixed-time control theory, a feedback compensation control scheme based on the fixed-time observer is proposed for the tracking problem of AGVs. Compared with the method suggested in the reference [17], the dwell time can be chosen independently of initial conditions

This paper is organized as follows. Section System Modeling and the Objective explains the modeling of autonomous ground vehicles and the objective. Section Main Results contains the time-varying yaw guidance law, state transformations, trajectory tracking control framework, and convergence analysis. Numerical simulations and discussions are presented in Section Simulation.

2. System Modeling and the Objective

2.1. System Modeling. The configuration of the AGV (i.e., the position and orientation) investigated in this paper can be described by two independent coordinates or two degrees of freedom, i.e., surge and yaw. For such AGVs, an inertial frame is used, as depicted in Figure 1. The states x, y, and φ are the longitudinal, lateral positions, and the vehicle's yaw angle in inertial coordinate, respectively. According to the existing literature [4], the kinematic and kinetic model of the AGV can be described as follows:

$$\begin{aligned} \dot{x} &= v_x \cos\varphi - v_y \sin\varphi, \\ \dot{y} &= v_x \sin\varphi + v_y \cos\varphi, \\ \dot{\varphi} &= w_r, \\ m\left(\dot{v}_y + v_x w_r\right) &= F_{yf} + F_{yr}, \\ I_z \dot{w}_r &= L_f F_{yf} - L_r F_{yr}. \end{aligned} \tag{1}$$

The states v_x, v_y, and w_r denote the vehicle's longitudinal, lateral, and yaw rate. The parameter m is the mass of the vehicle; F_{yf} and F_{yr} indicate the equivalent lateral forces of the front and rear axles, respectively. Parameters L_f and L_r are the distances from the C.G. to the front and rear axle, and I_z is the yaw moment of inertia. On the basis that the steering angle is sufficiently slight, the front and rear wheel lateral forces can be linearized below [18]:

$$\begin{aligned} F_{yf} &= -C_f a_f = -C_f\left(\beta + \frac{w_r L_f}{v_x} - \delta_f\right), \\ F_{yr} &= -C_r \mathrm{a}_r = -C_r\left(\beta - \frac{w_r L_r}{v_x}\right), \end{aligned} \tag{2}$$

where C_f and C_r denote the equivalent lateral stiffness of the front and rear axle, δ_f is the steering angle of the front wheel, a_f and a_r represent the sideslip angle of the front and rear wheels, and β is the sideslip angle.

In addition, due to the mechanical limitations of the vehicle itself, dead zones are commonly observed in servo valves or DC servo motors of AGVs. Hence, by combining (1)-(2) with the actuator dead-zone characteristic, the

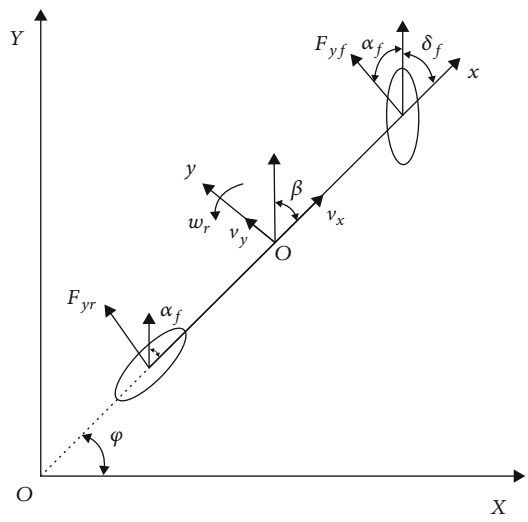

Figure 1: AGV model.

nonlinear model of the AGV considered in this paper is described as follows:

$$\begin{aligned}\dot{x} &= v_x \cos\varphi - v_y \sin\varphi,\\ \dot{y} &= v_x \sin\varphi + v_y \cos\varphi,\\ \dot{\varphi} &= w_r,\\ \dot{v}_y &= \Delta(v_y, w_r, t),\\ \dot{w}_r &= f(v_x, w_r, t) + L_f C_f I_z^{-1}\tau(\delta_f),\end{aligned} \tag{3}$$

where $\Delta(v_y, w_r, t) = -v_x w_r + m^{-1}[C_f(\tau(\delta_f) - \beta - v_x^{-1}w_x L_f) + C_r(v_x^{-1}w_r L_r - \beta)]$ and $f(v_x, w_r, t) = L_r C_r I_z^{-1}(\beta - v_x^{-1}w_r L_r) - L_f C_f I_z^{-1}(v_x^{-1}w_r L_f + \beta)$ are unknown unmodeled dynamics and disturbances and the input $\tau(\delta_f)$ is the force with the dead-zone nonlinearities, which can be described by

$$\tau(\delta_f) = \begin{cases} a_r(t)[\delta_f - b_r(t)], & \delta_f \geq b_r(t)\\ 0, & -b_l(t) < \delta_f < b_r(t),\\ a_l(t)[\delta_f + b_l(t)], & \delta_f \leq -b_l(t)\end{cases} \tag{4}$$

where $a_r(t)$, $a_l(t)$, $b_r(t)$, and $b_l(t)$ are positive constants satisfying the condition that $a_r(t) \geq \underline{a}_r$, $a_l(t) \geq \underline{a}_l$, $b_r(t) \leq \bar{b}_r$, and $b_l(t) \leq b_l$. In addition, $\underline{a}_r$, $\underline{a}_l$, b_r, and b_l are known positive constants.

2.2. The Objective. Define the reference trajectory as follows:

$$\begin{aligned}\dot{x}_{\text{ref}} &= v_{x,\text{ref}} \cos\varphi_{\text{ref}} - v_{y,\text{ref}} \cos\varphi_{\text{ref}},\\ \dot{y}_{\text{ref}} &= v_{x,\text{ref}} \sin\varphi_{\text{ref}} + v_{y,\text{ref}} \sin\varphi_{\text{ref}},\\ \dot{\varphi}_{\text{ref}} &= w_{\text{ref}},\end{aligned} \tag{5}$$

where x_{ref} and y_{ref} are the desired longitudinal and lateral positions and $v_{x,\text{ref}}$ and $v_{y,\text{ref}}$ are the desired longitudinal and lateral velocities, respectively. φ_{ref} and w_{ref} are the desired yaw angle and yaw angle rate of the vehicle, respectively. By analyzing system (3), the trajectory tracking problem can be transformed into the yaw angle tracking control problem by constructing the desired yaw angle φ_{ref} [4], which eventually satisfies $\varphi \longrightarrow \varphi_{\text{ref}}$.

Define the error states $x_e = x - x_{\text{ref}}$, $y_e = y - y_{\text{ref}}$, and $\varphi_e = \varphi - \varphi_{\text{ref}}$. Subsequently, the derivative of the position errors can be calculated as follows:

$$\begin{aligned}\dot{x}_e &= v_x \cos\varphi - v_{x,\text{ref}} \cos\varphi_{\text{ref}} - v_y \sin\varphi + v_{y,\text{ref}} \sin\varphi_{\text{ref}},\\ \dot{y}_e &= v_x \sin\varphi - v_{x,\text{ref}} \sin\varphi_{\text{ref}} + v_y \cos\varphi - v_{y,\text{ref}} \cos\varphi_{\text{ref}},\\ \dot{\varphi}_e &= w_r - w_{\text{ref}}.\end{aligned} \tag{6}$$

This paper is aimed at establishing a control methodology that can stabilize the trajectory tracking error system in (6) while ensuring that all closed-loop signals are bounded.

Remark 1. The trajectory tracking problem is transformed into the yaw angle tracking control problem, and it is efficient to reduce the complexity of controller design by dimension reduction. Due to the dead-zone nonlinearities of the input $\tau(\delta_f)$, the existing fixed-time observers for disturbance estimation cannot be applied directly, which increases the challenge of the tracking problem.

3. Main Results

3.1. Guidance Law Design. Define the coordinate transformation as follows:

$$z_1 = x_e \cos\varphi + y_e \sin\varphi, z_2 = -x_e \sin\varphi + y_e \cos\varphi. \tag{7}$$

The dynamics of $[z_1, z_2]$ can be stated as

$$\begin{aligned}\dot{z}_1 &= v_x - v_{x,\text{ref}} \cos\left(\varphi - \varphi_{ref}\right) - v_{y,\text{ref}} \sin\left(\varphi - \varphi_{\text{ref}}\right) + z_2 w_r,\\ \dot{z}_2 &= v_{x,\text{ref}} \sin\left(\varphi - \varphi_{ref}\right) - v_{y,\text{ref}} \cos\left(\varphi - \varphi_{ref}\right) - z_1 w_r + v_y.\end{aligned} \tag{8}$$

Lemma 2. *Stabilization of the system $[z_1, z_2]$ equals stabilizing the system $[x_e, y_e]$ in (6).*

Proof. The Jacobian matrix between $[z_1, z_2]$ and $[x_e, y_e]$ is $\begin{bmatrix}\cos\varphi & \sin\varphi\\ -\sin\varphi & \cos\varphi\end{bmatrix}$, whose rank is 2. This issue implies that the model transformation is differential homeomorphic. Additionally, the convergence of states z_1 and z_2 means the system $[x_e, y_e]$ converges to zero. In summary, stabilization of the system $[z_1, z_2]$ equals that stabilization of the system $[x_e, y_e]$. The proof is completed.□ □

The above lemma indicates that the trajectory tracking problem is to design desired yaw angle φ_{ref} to stabilize the system $[z_1, z_2]$.

Remark 3. In literature [4], the tanh $(\cdot)$ function is introduced to stabilize the error system, which is a standard method. However, in the system (8), due to the existence of undesired terms $-z_1 w_r + v_y$ involved in the error dynamic of z_2, the traditional method cannot be applied directly to stabilize the system (8). Hence, the desired yaw angle φ_{ref} should be redesigned.

In this paper, a novel idea of designing φ_{ref} stemming from the line of sight method is proposed, and a time-varying parameter ϵ is introduced to deal with the undesired terms involved in the error dynamic of z_2.

Lemma 4. *The state z_2 in (8) is stabilized if the following condition holds,*

$$\Delta^2 \le \left|\frac{1}{\chi}\right| \cdot |z_2| \cdot |1+\chi| = \left|\frac{1+\chi}{\chi}\right| \cdot |z_2|, \tag{9}$$

where Δ is the line of sight range, the variables $\chi = \Gamma^2 - 1$, $\Gamma^2 = v_{x,ref}^2 / f_{z2}^2$, and $f_{z2} = -z_1 w_r + v_y$.

Proof. To stabilize state z_2 while overcoming the term $-z_1 w_r + v_y$, we introduce the time-varying parameter ϵ based on the line of sight method, which satisfies $\varphi - \varphi_{ref} = -\arctan((z_2+\epsilon)/\Delta)$. Substituting $\varphi - \varphi_{\text{ref}}$ into equation (8), it gives

$$\begin{aligned}\dot{z}_2 &= -v_{x,\text{ref}} \frac{z_2+\epsilon}{\Delta^2 + (z_2+\epsilon)^2} + f_{z2} = -v_{x,\text{ref}} \frac{z_2}{\Delta^2 + (z_2+\epsilon)^2} \\ &\quad - v_{x,\text{ref}} \frac{\epsilon}{\Delta^2 + (z_2+\epsilon)^2} + f_{z2},\end{aligned} \tag{10}$$

where $-v_{y,\text{ref}} \cos(\varphi - \varphi_{\text{ref}}) + v_y$ is replaced by f_{z2} to simplify. In order to stabilize state z_2, the following condition eliminates the last second terms in (10):

$$f_{z2} = v_{x,\text{ref}} \frac{\epsilon}{\Delta^2 + (z_2+\epsilon)^2}, \tag{11}$$

then the value of the variable ϵ can be solved as

$$\epsilon = \frac{2z_2 - \sqrt{4z_2^2 + 4(\Delta^2 + z_2^2)(\Gamma^2 - 1)}}{2(\Gamma^2 - 1)}. \tag{12}$$

The solution $\epsilon = (2z_2 + \sqrt{4z_2^2 + 4(\Delta^2 + z_2^2)(\Gamma^2 - 1)})/2(\Gamma^2 - 1)$ is deleted because ϵ goes to infinity as $\Gamma^2 - 1 \longrightarrow 0$. Simultaneously, to ensure the existence of the value ϵ, the formula $4z_2^2 + 4(\Delta^2 + z_2^2)(\Gamma^2 - 1)$ under the root sign should be greater than or equal to 0, that is to say, $(\Gamma^2 - 1)\Delta^2 \ge -[z_2^2 + (\Gamma^2 - 1)z_2^2]$. Define $\chi = \Gamma^2 - 1$ for simplification, it gives

$$\chi\Delta^2 \ge -\left(z_2^2 + \chi z_2^2\right), \tag{13}$$

then the following conditions are discussed:

(1) If $\chi \ge 0$, that is to say, $|v_{x,\text{ref}}| \ge |f_{z2}|$, equation (13) is satisfied for any Δ

(2) If $-1 < \chi < 0$, that is to say, $|v_{x,\text{ref}}| < |f_{z2}|$, then $\Delta^2 \le -z_2(1+\chi)/\chi$ should be satisfied to guarantee equation (13)

(3) If $\chi < -1$, due to $\chi = \Gamma^2 - 1$, there is no solution Δ satisfying the condition (13)

In summary, the parameter Δ is chosen based on the condition (9). The proof is completed.□ □

The longitudinal velocity v_x is always sufficiently large in practice, which results that the absolute value of speed v_x is always more significant than that of term f_{z2}; then, Δ can be chosen without limitation. According to equations (8), (10), and (11), the derivative of $[z_1, z_2]$ yields:

$$\begin{aligned}\dot{z}_1 &= v_x - v_{x,\text{ref}} \cos(\varphi - \varphi_{\text{ref}}) - v_{y,\text{ref}} \sin(\varphi - \varphi_{\text{ref}}) + z_2 w_r, \\ \dot{z}_2 &= -v_{x,\text{ref}} \frac{z_2}{\Delta^2 + (z_2+\epsilon)^2}.\end{aligned} \tag{14}$$

Thus, to make the vehicle perfectly follows the reference trajectory, we only need to design the velocity v_x to stabilize z_1.

Lemma 5. *If the longitudinal velocity v_x satisfies that*

$$v_x = v_{x,ref} \cos\left(\varphi - \varphi_{ref}\right) - \kappa_u \tanh(z_1) - z_2 w_r - v_{y,ref} \sin\left(\varphi - \varphi_{ref}\right), \tag{15}$$

where the parameter k_u is a positive value, then the system $[z_1, z_2]$ in (8) converges to zero.

Proof. Substituting (15) into (8), the dynamics of z_1 and z_2 can be given as

$$\begin{aligned}\dot{z}_1 &= -\kappa_u \tanh(z_1), \\ \dot{z}_2 &= -v_{x,\text{ref}} \frac{z_2}{\Delta^2 + (z_2+\epsilon)^2}.\end{aligned} \tag{16}$$

States z_1 and z_2 converge to zero with $t \longrightarrow \infty$.□ □

In the after parts, we assume that longitudinal velocity has been closed-loop controlled and focuses on maintaining the yaw angle φ of the AGV on the desired value.

3.2. Improved Fixed-Time Disturbance Observer. In this subsection, a fixed-time disturbance observer considering inputs

dead-zones is proposed. In [4], the ARDC method is utilized to estimate the uncertainties and disturbances; however, the estimation error converges to zero asymptotically. The fixed-time control method has a faster convergence speed, and the settling time is dependent on the initial conditions. This issue prohibits its applicability in practical vehicle systems.

Define the desired yaw angle of AGV as $\varphi_d = -\arctan((z_2 + \epsilon)/\Delta) + \varphi_{\text{ref}}$, and the error of yaw angle and its derivative are $\epsilon_1 = \varphi - \varphi_d$ and $\epsilon_2 = \dot{\varphi} - \dot{\varphi}_d$. Then, one has

$$\begin{aligned} \dot{\epsilon}_1 &= \dot{\varphi} - \dot{\varphi}_d = \epsilon_2, \\ \dot{\epsilon}_2 &= \ddot{\varphi} - \ddot{\varphi}_d = f(v_x, w_r, t) - \ddot{\varphi}_d + g\tau(\delta_f), \end{aligned} \tag{17}$$

where $f(v_r, w_r, t)$ refers to the unknown unmodeled dynamics and disturbances, the parameter $g = L_f C_f I_z^{-1}$ is known, and the input $\tau(\delta_f)$ owns the dead-zone characteristic.

Assumption 6. The unknown term $\dot{f}(v_y, w_r, t)$ is bounded and satisfies $\dot{f}(v_y, w_r, t) = \Delta_f < \sigma$ with σ being a positive constant.

Then, the yaw angle tracking problem can be transformed to stabilize the system (17). To facilitate the subsequent analysis process, we introduce the definition of fixed-time control from [19–21].

Definition 7. Consider a system as

$$\dot{x} = g(t, x), x(0) = x_0, \tag{18}$$

where $x \in R^n$ is the state vector and $g : R^+ \times R^n$ is the nonlinear function. The system (18) is said to be fixed-time stable, if it is globally asymptotically stable and any solution $x(t, x_0)$ reaches the equilibria at some fixed-time moment, i.e., $x(t, x_0) = 0$, $\forall t \geq T(x_0)$, where $T : R^n \longrightarrow R^+ \cup \{0\}$ is the settling-time function.

Following the above definition, we define $\hat{\epsilon}_2$ and $\hat{f}(v_y, w_r, t)$ as the estimations of states ϵ_2 and $f(v_x, w_r, t)$ in (17), and the symbol $\lfloor \cdot \rceil^q$ as sign $(\cdot)|\cdot|^q$. Then, the fixed-time disturbance observer is developed based on system (17) as follows:

$$\begin{aligned} \dot{\hat{\epsilon}}_2 &= -\ddot{\varphi}_d + \hat{f}(v_y, w_r, t) + \kappa_{\tilde{\epsilon}_1} \lfloor \tilde{\epsilon}_2 \rceil^{1/2} + \kappa_{\tilde{\epsilon}_2} \lfloor \tilde{\epsilon}_2 \rceil^{p_\epsilon} \\ &\quad + \bar{a}(|\delta_f(t)| + \bar{b}) \text{Sign}(\tilde{\epsilon}_2) + \underline{\tau}, \\ \dot{\hat{f}}(v_x, w_r, t) &= \kappa_{\tilde{\epsilon}_3} \text{Sign}(\tilde{\epsilon}_2), \end{aligned} \tag{19}$$

where $p_\epsilon > 1$, $\bar{a} > \max\{a_l - \underline{a}_l, a_r - \underline{a}_r\}$, $\bar{b} > \max\{b_l - \underline{b}_l, b_r - \underline{b}_r\}$, and $\tilde{\epsilon}_2 = \epsilon_2 - \hat{\epsilon}_2$, $\underline{\tau}$ is

$$\underline{\tau} = \frac{\text{Sign}[\delta_f(t)]}{2} \{\text{Sign}[\delta_f(t)](\underline{\tau}_a + \underline{\tau}_b) - \underline{\tau}_a + \underline{\tau}_b\}, \tag{20}$$

with $\underline{\tau}_a = \underline{a}_r[\delta_f(t) - \underline{b}_r]$, and $\underline{\tau}_b = \underline{a}_l[\delta_f(t) + b_l]$. The constants $\kappa_{\tilde{\epsilon}_1}$, $\kappa_{\tilde{\epsilon}_2}$, and $\kappa_{\tilde{\epsilon}_3}$ satisfy

$$\kappa_{\tilde{\epsilon}_1} > \sqrt{2\kappa_{\tilde{\epsilon}_3}}, \kappa_{\tilde{\epsilon}_2} > 0, \kappa_{\tilde{\epsilon}_3} > 4\sigma. \tag{21}$$

Due to the existence of dead zones, the complete control signal cannot be obtained. So the traditional fixed or finite time observer cannot be directly applied. This section introduces the compensation term $\bar{a}(|\delta_f(t)| + \bar{b})\text{Sign}(\tilde{\epsilon}_2)$ more significant than $|\tau(\delta_f) - \underline{\tau}|$ to overcome the influence of the dead-zone characteristic on the observer design in (19).

Lemma 8. *Consider system (17) under Assumption 6, the observer (19) can estimate the term $f(v_x, w_r, t)$ within the fixed time.*

Proof. Define the estimation errors $\tilde{f}(v_x, w_r, t) = f(v_x, w_r, t) - \hat{f}(v_x, w_r, t)$ and $\tilde{\epsilon}_2 = \epsilon_2 - \hat{\epsilon}_2$. According to the system (19), we can have the derivatives of $\tilde{f}(v_x, w_r, t)$ and $\tilde{\epsilon}_2$ as follows:

$$\begin{aligned} \dot{\tilde{\epsilon}}_2 &= \tilde{f}(v_x, w_r, t) - \kappa_{\tilde{\epsilon}_1} \lfloor \tilde{\epsilon}_2 \rceil^{1/2} - \kappa_{\tilde{\epsilon}_2} \lfloor \tilde{\epsilon}_2 \rceil^{p_1} + g(\tau[\delta_f(t)] \\ &\quad - \underline{\tau}) - g(\bar{a}(|\delta_f(t)| + \bar{b})) \text{Sign}\left(\tilde{f}(v_x, w_r, t)\right), \\ \dot{\tilde{f}}(v_x, w_r, t) &= -\kappa_{\tilde{\epsilon}_3} \text{Sign}(\tilde{\epsilon}_2) + \Delta_f. \end{aligned} \tag{22}$$

Since $\Delta_f < \sigma$ and $\kappa_{\tilde{\epsilon}_3} > 4\sigma$, according to the Corollary 1 of [22], the estimation error $\tilde{f}(v_x, w_r, t)$ converges to zero in the fixed settling time:

$$\begin{aligned} T_{\tilde{\epsilon}} \leq &\left[\frac{1}{\kappa_{\tilde{\epsilon}_2}(p_\epsilon - 1)\left(2^{1/4}\kappa_{\tilde{\epsilon}_1}/\kappa_{\tilde{\epsilon}_2}\right)^{(p_\epsilon - 1)/(p_\epsilon + 1/2)}} \right. \\ &\left. + \frac{2\left(2^{3/4}\kappa_{\tilde{\epsilon}_1}/\kappa_{\tilde{\epsilon}_2}\right)^{1/2}}{\kappa_{\tilde{\epsilon}_1}} \right] \left[1 + \frac{\kappa_{\tilde{\epsilon}_3} + \sigma}{\left(\kappa_{\tilde{\epsilon}_3} - \sigma\right)\left(1 - \sqrt{2\kappa_{\tilde{\epsilon}_3}}/\kappa_{\tilde{\epsilon}_1}\right)} \right]. \end{aligned} \tag{23}$$

The proof is completed.□ □

3.3. Controller Design. The trajectory tracking control strategy is designed based on the fixed-time observer in this subsection. Consider the above disturbance observer (19), the system (17) with dead-zone characteristics can be described as following second-order nonlinear form:

$$\begin{aligned} \dot{\epsilon}_1 &= \epsilon_2, \\ \dot{\epsilon}_2 &= \hat{f}(v_x, w_r, t) + g\tau(\delta_f) + \tilde{f}(\varphi, w_r, t) - \ddot{\varphi}_d, \end{aligned} \tag{24}$$

where $\hat{f}(v_x, w_r, t)$ is the estimation of $f(v_x, w_r, t)$.

For the second-order nonlinear system (24), the control law in this subsection is designed as follows:

$$\delta_f = \begin{cases} -\frac{1}{a_l g}\left(\left|\widehat{f}(v_x, w_r, t) + \epsilon_{3*}\right|\right) - \bar{b}_l, & \xi_2 > 0, \\ 0, & \xi_2 = 0, \\ \frac{1}{a_r g}\left(\left|\widehat{f}(v_x, w_r, t) + \epsilon_{3*}\right|\right) + \bar{b}_r, & \xi_2 < 0, \end{cases} \tag{25}$$

where variables ξ_1 and ξ_2 are

$$\xi_1 = \beta_1 \lfloor \epsilon_1 \rceil^{q_1} + \lfloor \epsilon_2 \rceil^{1/\lambda} + \beta_2 \lfloor \epsilon_1 \rceil^{q_2}, \xi_2 = \lfloor \xi_1 \rceil^{\lambda} + \epsilon_2, \tag{26}$$

and variable ϵ_{3*} is

$$\begin{aligned} \epsilon_{3*} = &\left(\beta_3 \lfloor \xi_2 \rceil^{q_3} + \beta_4 \lfloor \xi_2 \rceil^{q_4} + \beta_1 \lambda q_1 |\xi_1|^{\lambda-1} |\epsilon_1|^{q_1-1} \epsilon_2 \right. \\ &\left. + \beta_2 \lambda q_2 |\xi_1|^{\lambda-1} \times |\epsilon_1|^{q_2-1} \epsilon_2\right)\left(1 + |\xi_1|^{\lambda-1} |\epsilon_2|^{(1/\lambda)-1}\right)^{-1}, \end{aligned} \tag{27}$$

where $\lambda = 0.5$, $1 < q_1 < 2, q_2 > 2, 0 < q_3 < 1, q_4 > 1$, β_1, β_2, β_3, β_4 are designed positive constants.

Lemma 9. *The control law (25) can ensure that the system (24) converges to zero in fixed time with the settling time T_c, where:*

$$T_c = \frac{2^{(1-q_3)/2}}{\beta_3(1-q_3)} + \frac{2^{(1-q_4)/2}}{\beta_4(q_4-1)} + \frac{2^{\lambda}}{\beta_1^{\lambda}(1-\lambda q_1)} + \frac{2^{\lambda}}{\beta_2^{\lambda}(\lambda q_2 - 1)}. \tag{28}$$

Proof. Since $\tilde{f}(v_x, w_r, t)$ converges to zero in fixed time with Lemma 8, for any $t > T_{\bar{\epsilon}}$, the dynamics of states ϵ_1 and ϵ_2 in (24) can be represented as:

$$\begin{aligned} \dot{\epsilon}_1 &= \epsilon_2, \\ \dot{\epsilon}_2 &= \widehat{f}(v_r, w_r, t) + g\tau(\delta_f) - \ddot{\varphi}_d. \end{aligned} \tag{29}$$

According to results in [22], the system (29) converges to zero before the fixed time $T_s = T_c + T_{\bar{\epsilon}}$. The proof is completed.□ □

In the above theorem, the state transformation is introduced:

$$\xi_2 = \lfloor \xi_1 \rceil^{\lambda} + \epsilon_2, \tag{30}$$

which guarantees the nonsingularity of the control law. This characteristic can be directly derived from the nonsingularity of ϵ_{3*}. By the definition of ϵ_{3*}, we can know:

$$\begin{aligned} \epsilon_{3*} = &\left(\beta_3 \lfloor \xi_2 \rceil^{q_3} + \beta_4 \lfloor \xi_2 \rceil^{q_4} + \beta_1 \lambda q_1 |\xi_1|^{\lambda-1} |\epsilon_1|^{q_1-1} \epsilon_2 \right. \\ &\left. + \beta_2 \lambda q_2 |\xi_1|^{\lambda-1} |\epsilon_1|^{q_2-1} \epsilon_2\right) \times \left(1 + |\xi_1|^{\lambda-1} |\epsilon_2|^{(1/\lambda)-1}\right)^{-1}. \end{aligned} \tag{31}$$

Moreover, we have

$$\begin{aligned} \epsilon_{3*} = &|\xi_1|^{1-\lambda}\left(\beta_3 \lfloor \xi_2 \rceil^{q_3} + \beta_4 \lfloor \xi_2 \rceil^{q_4}\right)\left(|\xi_1|^{1-\lambda} + |\epsilon_2|^{(1/\lambda)-1}\right)^{-1} \\ &+ \beta_1 \lambda q_1 |\epsilon_1|^{q_1-1} \epsilon_2 \times \left(|\xi_1|^{1-\lambda} + |\epsilon_2|^{(1/\lambda)-1}\right)^{-1} \\ &+ \beta_2 \lambda q_2 |\epsilon_1|^{q_2-1} \epsilon_2 \left(|\xi_1|^{1-\lambda} + |\epsilon_2|^{(1/\lambda)-1}\right)^{-1}, \end{aligned} \tag{32}$$

with parameter $\lambda = 0.5$, hence, one has $|\xi_1|^{1-\lambda}(|\xi_1|^{1-\lambda} + |\epsilon_2|^{(1/\lambda)-1})^{-1} = |\xi_1|^{0.5}(|\xi_1|^{0.5} + |\epsilon_2|^{(1/\lambda)-1})^{-1} \le 1, |\epsilon_2|(|\xi_1|^{1-\lambda} + |\epsilon_2|^{(1/\lambda)-1})^{-1} = |\epsilon_2|(|\xi_1|^{1-\lambda} + |\epsilon_2|)^{-1} \le 1$. Then, ϵ_{3*} must be a nonsingular variable; hence, the control law (25) is also nonsingular.

According to Lemma 9, the proposed control law can stabilize the second-order nonlinear system (17) with the actuators' dead zones in the fixed-time. Finally, the trajectory tracking control theorem for AGVs with dead zones is given.

Theorem 10. *Consider the AGV dynamics in (1)-(3) with the dead zones (4), combining with the fixed-time state observer (19) and the control law (25). Under Assumption 6, the error signals $\tilde{f}(v_x, w_r, t)$, ϵ_1, and ϵ_2 in the closed-loop system for the trajectory tracking control of the AGV have bounded in the fixed time T_s. Besides, the trajectory tracking control can be achieved.*

Proof. According to Lemmas 8 and 9, the fixed-time state observer (19) and the control law (25) can stabilize the transformed system in the fixed time. With Lemmas 2–5, the trajectory tracking control can be proved.□ □

4. Simulation

To verify the effectiveness of the presented method, we use CarSim and MATLAB platforms to carry out the trajectory tracking problem. We used a general AGV model derived by [4]. In this simulation, the proposed guidance laws (9), fixed-time state observer (19), and the control law (25) are applied. Let the AGV have the following initial conditions: $[x(0), y(0), \varphi(0), v_x(0), v_y(0), w_r(0)]^T = [0, 0, 0, 0, 0, 0]^T$, representing the initial values of positions x and y, yaw angle φ, velocities v_x, v_y, and yaw angle rate w_r, respectively. The reference trajectory is chosen as $[x_d(0), y_d(0)] = [10m, 10m]$, $\varphi_d = 0.15 \sin(0.1 \times t)$.

Table 1 shows all the variables involved in the AGV model. The parameters of actuator dead-zones and control

Table 1: The model parameters of the AGV.

Symbol	Quantity	Value
m	Mass of the vehicle	1723 kg
I_z	Vehicle yaw moment of inertial	4175 kg·m
L_f	The distances from vehicle C.G. to the front axis center	1.232 m
L_r	The distances from vehicle C.G. to the rear axis center	1.468 m
C_f	Vehicle nominal front axle cornering stiffness	N/rad
C_r	Vehicle nominal rear axle cornering stiffness	N/rad

parameters are chosen as follows:

$$a_r = 0.7 + 0.3|\sin t|, a_l = 0.7 + 0.3|\sin t|, b_r = 5 + 5|\cos t|, b_l = 5 + 5|\cos t|,$$
$$\kappa_{\bar{\varepsilon}_1} = 2, \kappa_{\bar{\varepsilon}_2} = 0.3, \kappa_{\bar{\varepsilon}_3} = 2, p_1 = 2,$$
$$q_1 = 1.9, q_2 = 2.1, q_3 = 0.9, q_4 = 1.1, \beta_1 = 0.2, \beta_2 = 2, \beta_3 = 0.2, \beta_4 = 2,$$
$$\bar{a}_r = 1, \bar{a}_l = 1, \underline{a}_l = 0.7, \underline{a}_l = 0.7, \bar{b}_l = 10, \bar{b}_l = 10, \underline{b}_l = 5, \underline{b}_l = 5. \tag{33}$$

4.1. Disturbance Observer Compensation. To illustrate the advantage of the proposed disturbance observer, the trajectories of our improved disturbance observer and conventional fixed-time disturbance observer are shown in Figures 2 and 3.

In this comparison, we aim at the compensation result of the dead zone of the actuator in the improved fixed time disturbance observer (Improved-FTDO) and compare it with the conventional fixed time disturbance observer (FTDO) [17]. The results show that after considering the dead zone of the actuator, the improved FTDO method proposed is better than the conventional FTDO method because the compensation problem is considered in this paper.

4.2. Actuator Compensation. The simulation results are shown in Figures 4–7. To evaluate the effectiveness of our method, we consider the convergence comparisons between the control methods of ADCC and NTSM-ADRC in [4, 22], respectively. The same driving conditions are carried out, whose road adhesion coefficient is 0.8. We now look at the differences in the performance of yaw angle changing δ_f shown in Figures 4. It reveals that the maximum value of δ_f in our method is the minimum one in the three approaches, which means that the input of yaw angle changing δ_f is gentler than the other two controllers, and the ride comfort is guaranteed.

In Table 1, only the nominal values of the parameters are given, and there are still many parametric uncertainties. For example, (1) the tire deformation; (2) the equivalent lateral stiffness C_f and C_r of the front and rear axle change caused by wheel load transfer; (3) the shift in road attachment, and (4) the distance from the front and rear axles to the center of the vehicle L_f and L_r change caused by the vehicle's centroid position changes. Here, we consider the influence of the lateral stiffness values on the performance of the proposed control algorithm. We analyze the impact of the lateral stiffness

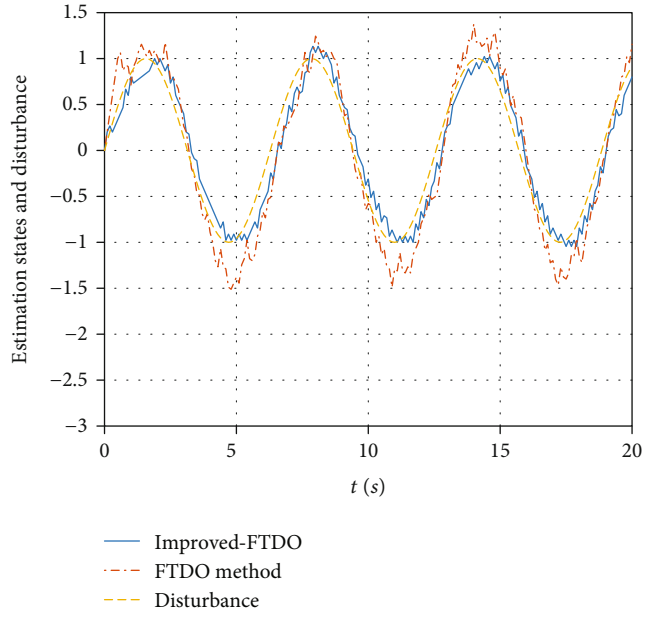

Figure 2: Comparisons of estimation states.

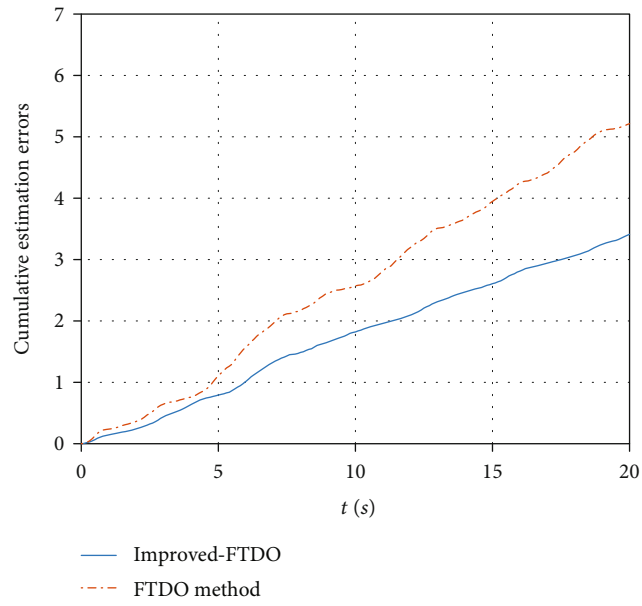

Figure 3: Comparisons of cumulative estimation errors.

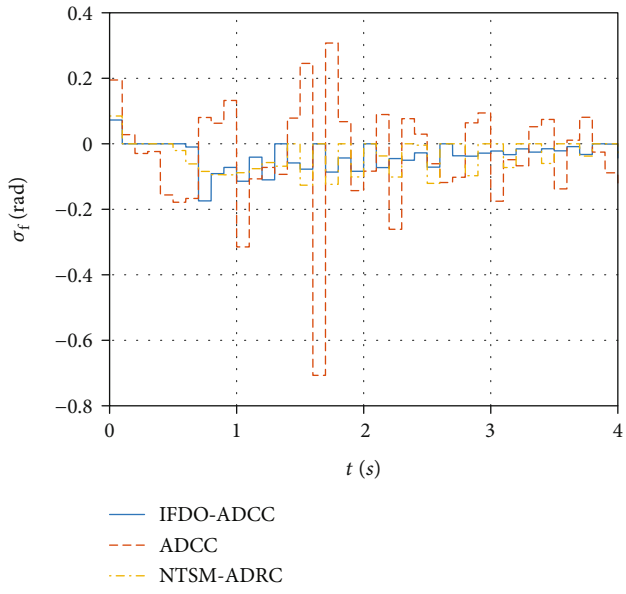

Figure 4: Comparisons of inputs.

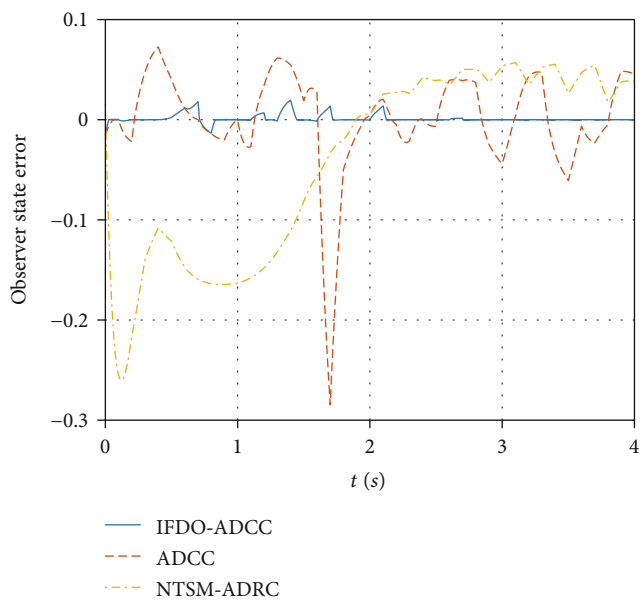

Figure 5: Comparisons of observer errors.

values with unknown values of C_f and C_r in simulations. The IFDO-ADCC does not need to set different control parameters for various vehicle speeds than some controllers. It has strong robustness to the change of the external environment.

Moreover, the IFDO-ADCC can dynamically estimate and compensate the system for total disturbances in fixed time. The simulation results are shown in Figure 5. We can see that the IFDO-ADCC has faster estimation error convergence and good disturbance estimation performance, which reflects the excellent robustness to the uncertainties. The trajectory tracking performances of AGVs by the controllers of IFDO-ADCC, ADCC, and NTSM-ARDC are given in

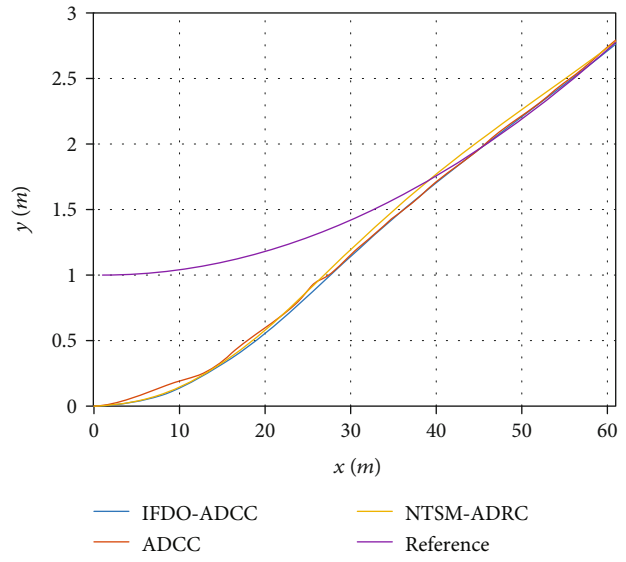

Figure 6: Comparisons of trajectories of positions.

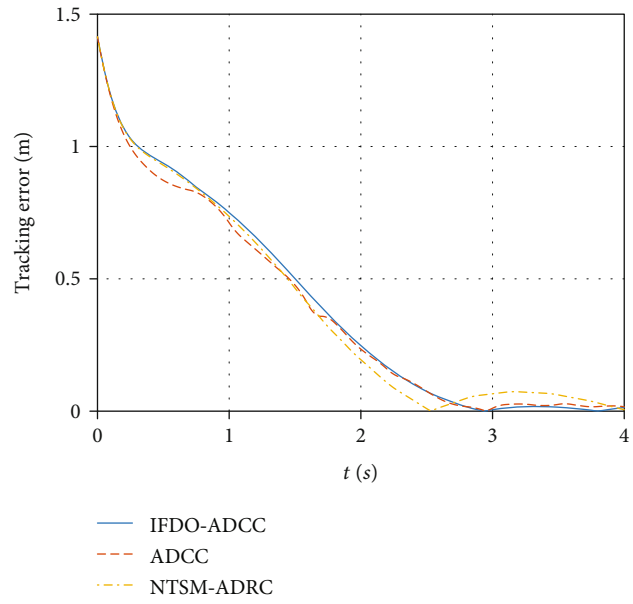

Figure 7: Comparisons of tracking errors.

Figure 6. We can see that three controllers can track the reference trajectory well. Figure 7 shows the corresponding tracking error of the vehicle under different controllers. It can be seen that the trajectory tracking performance of the proposed IFDO-ADCC method is superior to ADCC and NTSM-ARDC.

4.3. Overall Situation. In Figure 8, the CarSim and MATLAB simulation results of the trajectory tracking based on the proposed guidance laws (9), fixed-time state observer (19), and the control law (25) are given. It shows that the proposed algorithms can be applied in actual scenarios.

Compared with the ADCC method and NTSM-ARDC proposed in [4], the case of input dead zones is considered in the trajectory tracking performance in our paper.

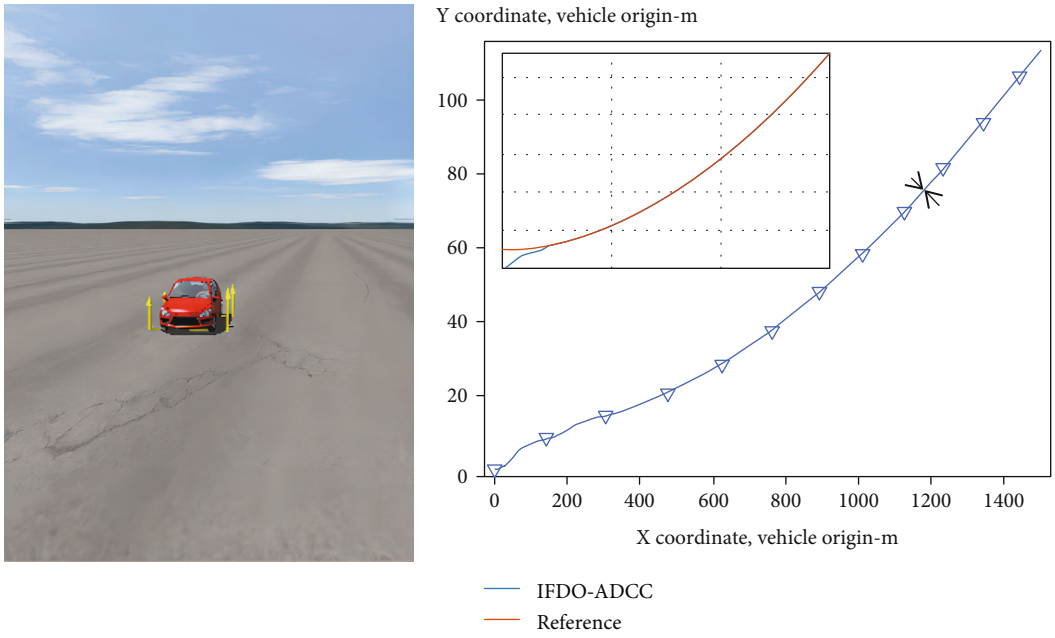

Figure 8: Trajectories of positions in MATLAB and CarSim platforms.

Although the control input falls in the dead-zone at a specific time when the actuator has no output signal, the performance in trajectory tracking errors is guaranteed, proving the effectiveness of the method proposed in our paper.

5. Conclusions

In this paper, based on a global diffeomorphism transformation, a fixed-time observer control method is proposed for the trajectory tracking problem of the AGV system. Trajectory tracking of AGVs subject to actuator saturation is still an open problem. Energy consumption optimal control of AGVs is another interesting problem to be studied in the future. Additionally, some nonlinear system control methods can also be applied for AGVs in the future. For example, an adaptive super-twisting sliding mode control technique is developed for forn-link rigid robotic manipulators [23]. An adaptive nonsingular integral-type second-order terminal sliding mode tracking control for nonlinear systems with uncertainties is proposed [24].

Data Availability

This paper uses MATLAB and CarSim cosimulation; if the reviewers need, the authors can upload the source file.

Conflicts of Interest

The authors declare that they have no conflicts of interest.

Acknowledgments

The supports of this paper are the Project Supported by Scientific Research Fund of Zhejiang Provincial Education Department under Grant Y202146005 and the General Projects of Science and Technology under Grant 2021XJKJ04.

References

[1] M. Elbanhawi, M. Simic, and R. Jazar, "The role of path continuity in lateral vehicle control," *Procedia Computer Science*, vol. 60, pp. 1289–1298, 2015.

[2] Y. Wu, L. Wang, J. Zhang, and F. Li, "Path following control of autonomous ground vehicle based on non-singular terminal sliding mode and active disturbance rejection control," *IEEE Transactions on Vehicular Technology*, vol. 60, no. 99, pp. 1–1, 2019.

[3] Z. H. O. N. G. P. I. N. G. Jiangdagger and H. Nijmeijer, "Tracking Control of Mobile Robots: A Case Study in Backstepping∗," *Automatica*, vol. 33, no. 7, pp. 1393–1399, 1997.

[4] J. Wang, J. Steiber, and B. Surampudi, "Autonomous ground vehicle control system for high-speed and safe operation," *International Journal of Vehicle Autonomous Systems*, vol. 7, no. 1/2, pp. 18–35, 2009.

[5] J. Guo, Y. Luo, and K. Li, "An adaptive hierarchical trajectory following control approach of autonomous four-wheel independent drive electric vehicles," *IEEE Transactions on Intelligent Transportation Systems*, vol. 19, no. 8, pp. 2482–2492, 2018.

[6] W. Kim, Y. S. Son, and C. C. Chung, "Torque-overlay-based robust steering wheel angle control of electrical power steering for a lane-keeping system of automated vehicles," *IEEE Transactions on Vehicular Technology*, vol. 65, no. 6, pp. 4379–4392, 2016.

[7] H. Jing, R. J. Wang, J. Wang, and N. Chen, "Robust H_{∞} dynamic output-feedback control for four- wheel independently actuated electric ground vehicles through integrated AFS/DYC," *Journal of the Franklin Institute*, vol. 355, no. 18, pp. 9321–9350, 2018.

[8] Y. Chen, Y. Cai, J. Zheng, and D. Thalmann, "Accurate and efficient approximation of clothoids using Bézier curves for path planning," *IEEE Transactions on Robotics*, vol. 33, no. 5, pp. 1242–1247, 2017.

[9] Z. Li, J. Deng, R. Lu, Y. Xu, J. Bai, and C. Y. Su, "Trajectory-tracking control of mobile robot systems incorporating neural-dynamic optimized model predictive approach," *IEEE Transactions on Systems Man and Cybernetics Systems*, vol. 46, no. 6, pp. 740–749, 2016.

[10] N. Gu, D. Wang, Z. Peng, and L. Liu, "Observer-based finite-time control for distributed path maneuvering of underactuated unmanned surface vehicles with collision avoidance and connectivity preservation," *IEEE Transactions on Systems, Man, and Cybernetics*, vol. 51, no. 8, pp. 1–11, 2019.

[11] K. Y. Pettersen and O. Egeland, "Exponential stabilization of an underactuated surface vessel," *Conference on Decision and Control*, vol. 1, no. 3, pp. 967–972, 1996.

[12] R. J. Diaz and R. Rosenberg, "Spreading dead zones and consequences for marine ecosystems," *Science*, vol. 321, no. 5891, pp. 926–929, 2008.

[13] W. Shi, H. Zhao, J. Ma, and Y. Yao, "Dead-zone compensation of an ultrasonic motor using an adaptive dither," *IEEE Transactions on Industrial Electronics*, vol. 65, no. 5, pp. 3730–3739, 2018.

[14] C. Chen, Y. Jia, M. Shu, and Y. Wang, "Hierarchical adaptive path-tracking control for autonomous vehicles," *IEEE Transactions on Intelligent Transportation Systems*, vol. 16, no. 5, pp. 2900–2912, 2015.

[15] L. Tang, F. Yan, B. Zou, K. Wang, and C. Lv, "An improved kinematic model predictive control for high-speed path tracking of autonomous vehicles," *IEEE Access*, vol. 8, pp. 51400–51413, 2020.

[16] X. Ji, Y. Liu, X. He et al., "Interactive control paradigm-based robust lateral stability controller design for autonomous automobile path tracking with uncertain disturbance: a dynamic game approach," *IEEE Transactions on Vehicular Technology*, vol. 67, no. 8, pp. 6906–6920, 2018.

[17] X. Yu, P. Li, and Y. Zhang, "The design of fixed-time observer and finite-time fault-tolerant control for hypersonic gliding vehicles," *IEEE Transactions on Industrial Electronics*, vol. 65, no. 5, pp. 4135–4144, 2018.

[18] K. Nam, S. Oh, H. Fujimoto, and Y. Hori, "Estimation of sideslip and roll angles of electric vehicles using lateral tire force sensors through rls and kalman filter approaches," *IEEE Transactions on Industrial Electronics*, vol. 60, no. 3, pp. 988–1000, 2013.

[19] A. Polyakov, "Nonlinear feedback design for fixed-time stabilization of linear control systems," *IEEE Transactions on Automatic Control*, vol. 57, no. 8, pp. 2106–2110, 2012.

[20] S. P. Bhat and D. S. Bernstein, "Finite-time stability of continuous autonomous systems," *SIAM Journal on Control and Optimization*, vol. 38, no. 3, pp. 751–766, 2000.

[21] Y. Orlov, "Finite time stability and robust control synthesis of uncertain switched systems," *SIAM Journal on Control and Optimization*, vol. 43, no. 4, pp. 1253–1271, 2004.

[22] P. Zhang and G. Guo, "Fixed-time switching control of underactuated surface vessels with dead-zones: global exponential stabilization - ScienceDirect," *Journal of the Franklin Institute*, vol. 357, no. 16, pp. 11217–11241, 2020.

[23] S. Mobayen and A. Fairouz, "Design of an adaptive tracker forn-link rigid robotic manipulators based on super-twisting global nonlinear sliding mode control," *International Journal of Systems Science*, vol. 48, no. 9, pp. 1990–2002, 2017.

[24] S. Mobayen, H. Karami, and A. Fekih, "Adaptive non-singular integral-type second order terminal sliding mode tracking controller for uncertain nonlinear systems," *International Journal of Control, Automation and Systems*, vol. 19, no. 4, pp. 1539–1549, 2021.